TOXICOLOGICAL SCIENCES **111(1)**, 37–48 (2009)
doi:10.1093/toxsci/kfp139
Advance Access publication July 2, 2009

Quantitative Determination of Skin Penetration of PEG-Coated CdSe Quantum Dots in Dermabraded but not Intact SKH-1 Hairless Mouse Skin

Neera V. Gopee,*,† Dean W. Roberts,*,† Peggy Webb,*,† Christy R. Cozart,* Paul H. Siitonen,* John R. Latendresse,‡ Alan R. Warbitton,‡ William W. Yu,§ Vicki L. Colvin,§ Nigel J. Walker,¶ and Paul C. Howard*,†,[1]

*National Center for Toxicological Research; †National Toxicology Program Center for Phototoxicology, U.S. Food & Drug Administration, Jefferson, Arkansas 72079; ‡Toxicology Pathology Associates, Jefferson, Arkansas 72079; §Center for Biological and Environmental Nanotechnology, Rice University, Houston, Texas 77005; and ¶National Toxicology Program, National Institute of Environmental Health Sciences, National Institutes of Health, Research Triangle Park, North Carolina 27709

Received March 15, 2009; accepted June 18, 2009

Many cosmetics, sunscreens, and other consumer products are reported to contain nanoscale materials. The possible transdermal absorption of nanoscale materials and the long-term consequences of the absorption have not been determined. We used polyethylene glycol coated cadmium selenide (CdSe) core quantum dots (QD; 37 nm diameter) to evaluate the penetration of nanoscale material into intact, tape stripped, acetone treated, or dermabraded mouse skin. QD were suspended in an oil-in-water emulsion (approximately 9μM) and the emulsion was applied at 2 mg/cm^2 to mouse dorsal skin pretreated as follows: intact; tape stripped to remove the stratum corneum; acetone pretreated; dermabraded to remove stratum corneum and epidermis. QD penetration into the skin was monitored in sentinel organs (liver and regional draining lymph nodes) using inductively coupled plasma mass spectrometry analysis of cadmium (from the CdSe QD). No consistent cadmium elevation was detected in the sentinel organs of mice with intact, acetone pretreated, or tape-stripped skin at 24- and 48-h post-QD application; however, in dermabraded mice, cadmium elevations were detected in the lymph nodes and liver. QD accumulation (as cadmium) in the liver was approximately 2.0% of the applied dose. The passing of QD through the dermabraded skin was confirmed using confocal fluorescence microscopy. These results suggest that transdermal absorption of nanoscale materials depends on skin barrier quality, and that the lack of an epidermis provided access to QD penetration. Future dermal risk assessments of nanoscale materials should consider key barrier aspects of skin and its overall physiologic integrity.

Key Words: **quantum dots; nanoscale materials; dermabrasion.**

Nanotechnology involves the manipulation of matter at the atomic or molecular scale, where the dimensions are less than 100 nm (Feynman, 1959; National Nanotechnology Initiative [NNI]; Oberdörster *et al.*, 2005). In an early treatise on the synthesis of nanomaterials, Whitesides *et al.* (1991) pointed out that synthesis in this size domain has been occurring for some time through (1) chemical synthesis of structures using covalent bonds; (2) covalent polymerization; (3) self-assembly of crystal and colloid structures through ionic, hydrogen bond, or van der Waals interactions; or (4) molecular self-assembly using combinations of the other synthetic approaches. The direct synthesis of nanoscale materials from atomic elements is referred to as a bottom-up approach, whereas the reduction of the size of larger particles of a particular material (e.g., micron sized) through mechanical means is referred to as a top-down approach. Regardless of which approach is used, the discovery and application of nanomaterials is one of the fastest growing fields of science today.

The synthesis of nanoscale materials is neither new nor entirely anthropogenic. Biological materials such as proteins, lipids, RNA, and DNA use ionic or hydrogen bonding to either self-orient or self-assembly into complex aggregates (Minetti and Remeta, 2006; Schneider *et al.*, 2007; Westhof and Hardy, 2004; White and Wimley, 1999). The crystallization of calcium phosphate (Randall's plaque) (Çiftçioğlu *et al.*, 2008), calcium oxalate (Robertson, 2004), and melamine cyanurate (Dobson *et al.*, 2008; Reimschuessel *et al.*, 2008; Whitesides *et al.*, 1991) that occurs in the renal tubules or urinary bladder is an additional example of the self-assembly at the nanoscale that occurs in biological systems. Other naturally occurring nanoscale materials that self-assemble include viruses (Zlotnick, 2005), magnetite (Arakaki *et al.*, 2008; Komeili, 2007), ferritin (Alekseenko *et al.*, 2008; Theil *et al.*, 2006), and fullerenes in geological residues (Busek, 2002; Busek *et al.*, 1992; Mossman *et al.*, 2003).

Anthropogenic nanomaterials are being commercialized for a wide range of applications in the fields of biotechnology, bioengineering, medicine, and materials science. The influx of funding from government sources, such as the U.S. NNI ($1.5 billion in 2009), and the focused efforts at the National

[1] To whom correspondence should be addressed at Division of Biochemical Toxicology, National Toxicology Program Center for Phototoxicology, National Center for Toxicological Research, U.S. Food & Drug Administration, 3900 NCTR Road, HFT-110, Jefferson, AK 72079. Fax: (870) 543-7136. E-mail: Paul.Howard@fda.hhs.gov.

Institutes of Health (NIH) to use nanotechnology to detect, diagnose, and treat disease have led to a virtual explosion in the development of nanotechnology-based materials (NCI; NIH; NNI). Some of these applications are refinements of old technologies, such as continued development of nanoscale superparamagnetic particles for magnetic resonance contrast imaging (Lee *et al*., 2007; Longmire *et al*., 2008; Sosnovik, 2008), the application of nanoscale titanium dioxide and zinc oxide as sunscreens (Hansen *et al*., 2008; Nohynek *et al*., 2007, 2008), and the use of nanoscale silver as an antimicrobial agent (Kim *et al*., 2007; Li *et al*., 2008; Rai *et al*., 2009). In the case of nanosilver, it is anticipated that a significant portion of the population could be exposed, based on the number of products being developed and marketed (> 230; Woodrow Wilson Institute, 2008) that contain nanoscale silver including wound dressings, textiles for clothing, air filters, toothbrushes and dentifices, air filters, vacuum cleaners, personal hygiene products, and washing machines (Luoma, 2008; Woodrow Wilson Institute, 2008).

Fluorescent quantum dots (QD) are typically composed of a nanoassembly of an inorganic metallic core (e.g., cadmium selenide, indium-gallium-arsenide), an insulating shell (e.g., zinc sulfide, cadmium sulfide), and an outer coating (Bhattacharya *et al*., 2004; Gao *et al*., 2005; Knight *et al*., 2004; Nirmal *et al*., 1996; Reimann and Manninen, 2002; Zheng *et al*., 2007). The market for QD technology (colloidal suspensions, optoelectronics, solar energy, electronics, and optics) was $29 million in 2008 and is expected to grow to $246 million by 2013 (Les, 2008). As a result of this increased use, there could potentially be increased exposure to QD during manufacture, product use, or product disposal.

A significant concern with the use of nanotechnology-based products is that nanoscale materials will penetrate protective physical barriers, such as the skin, lung, intestinal tract, and blood-brain barrier, and that the internalized nanomaterials will cause harm. The lack of quantitative information on the biological uptake of nanomaterials and toxicity of these materials has led to requests for moratoriums on marketing nanoscale materials until the full potential of transport and toxicology are understood (Bailey 2003; ETC, 2003, 2006; Miller, 2008).

In an attempt to address some of the concerns regarding nanomaterial safety, we have quantified the biological distribution of poly(ethylene glycol) (PEG)–coated QD following injection into skin in order to determine the biological distribution of the nanomaterials (Gopee *et al*., 2007). In this report we quantify the skin penetration of the PEG-coated QD in a hairless mouse model under conditions where the skin was intact or compromised.

MATERIALS AND METHODS

Synthesis and characterization of nanoscale CdSe quantum dots. The amine terminated, PEG-coated QD were prepared and characterized as previously described (Gopee *et al*., 2007). The QD consisted of a CdSe core and CdS shell and was nail-shaped (8.4 × 5.8 nm) with an emission maximum of 621 nm (Gopee *et al*., 2007). With the polymer coating, the QD were 37 ± 1 nm as determined by size exclusion chromatography and dynamic light scattering (Gopee *et al*., 2007). The concentration of QD was determined to be 19 ± 2.5μM as assessed by UV/VIS spectroscopy (Gopee *et al*., 2007). Inductively coupled plasma mass spectroscopy (ICP-MS) analysis of the QD solution demonstrated 38mM Cd and 6mM Se for a Cd:Se ration of 6.4:1 (Gopee *et al*., 2007).

Preparation of oil-in-water emulsion containing QD. An oil-in-water emulsion containing the water-soluble QD was made as follows. Part 1 of the emulsion was prepared by mixing 1 g of polyglyeryl-3 distearate (BASF, Parsipanny, NJ), 1 g cetearyl alcohol (Henkel Corp., Hoboken, NJ), and 3.33 g of mineral oil (USP, Penreco, Karns City, PA) at 60°C. Part 2 was made by mixing 16.7 mg of propylene glycol (Aldrich Chem. Co., Milwaukee, WI) with 0.4 ml of potassium phosphate, pH 7. Part 3 was made by mixing 10 mg methyl paraben (Pfaltz & Bauer, Inc., Stamford, CT), 10 mg of propyl paraben (Pfaltz & Bauer, Inc.), and 5 ml of water:propylene glycol (4:1) at 60°C. All parts were heated to 60°C, and Part 1 and 2 were mixed in a ratio of 1:2, respectively, at 1400 rpm using a heated mixer (Eppendorf Thermomixer) for 5 min, and then an equal volume of QD (or water) were added. Part 3 was added to give a ratio of 1:100 with the total mixture, and the solution was mixed briefly at 60°C, at 10 min at 40°C, followed by continued mixing until room temperature was achieved. The emulsion was used immediately for the studies. In these studies, the concentration of the QD was reduced from 19μM in the stock solution to 9.4μM in the emulsion.

Animals. Female isolator-reared hairless *Helicobacter*-free Crl: SKH-1 (hr^-/hr^-) mice were obtained from Charles River Corporation (Boston, MA) at 6 weeks of age. The mice were housed for 2 weeks in the NCTR Animal Quarantine Facility and acclimated in the animal room prior to use. The treatment of the mice conformed to Animal Care and Use Committee guidelines at this American Association for Laboratory Animal Care approved facility.

Treatment of mice and application of QD. At 9–12 weeks of age, the mice were weighed and anesthetized intraperitoneally with sodium pentobarbital (19 mg/kg body weight; Nembutal, Abbott Laboratories, North Chicago, IL). Mice were tape stripped 5–20 times on the right dorsal flank ($n = 4$ mice per group) using D-Squame Skin Sampling Discs, with an area of 3.8 cm^2 (CuDerm Corporation, Dallas, TX) applied to the right dorsal flank under ~47 g/cm^2 using a modified D-Squame pressure device (CuDerm Corporation) for 5 s. Dermabrasion ($n = 5$ mice) was accomplished using a small felt wheel attached to a hand-held motor as described by Trempus *et al*. (1998). A Dremel felt wheel (Dremel, Racine, WI) was attached to a Dremel 400XPR hand-held motor, and operated at 6000 rpm. The tool is held in one hand and lightly moved in one pass over the skin while the mouse skin is held taut with the other hand. This method was validated using histopathology examination of dermabraded skin during method development. Animals were pretreated once daily for four consecutive days with acetone wipes (Contec, Spartanburg, SC). Approximately 1.6 × 1.6 cm of skin on the dorsal lateral back of the mice was used for application of 5 μl of the QD emulsion. The area was either untreated or pretreated with acetone, tape stripping, or dermabrasion (24 h, < 5 min, or < 5 min, respectively) prior to the application of the QD. On some of the mice, the area containing the QD was covered with an occlusion patch (Hill Top Research, Inc., Miamiville, OH), which was held in place with adhesive tape. All mice were fitted with Elizabethan collars (Kong Veterinary Products., Irwindale, CA) to prevent grooming the site of application. Mice were euthanized and the skin was removed and placed in 10% neutral buffered formalin, and after 24 h was dehydrated with ethanol, embedded in paraffin blocks, sectioned at 4 μm, and stained with hematoxylin and eosin and examined by light microscopy, or and mounted onto slides without staining or cover slips for fluorescence microscopy.

The mice ($n = 4$ per treatment group) were sacrificed at 0, 24, and 48 h, and blood, liver, and regional draining lymph nodes were collected and analyzed by ICP-MS for cadmium and selenium. Tissues from one mouse at each time point were collected and processed for fluorescence microscopy (see above).

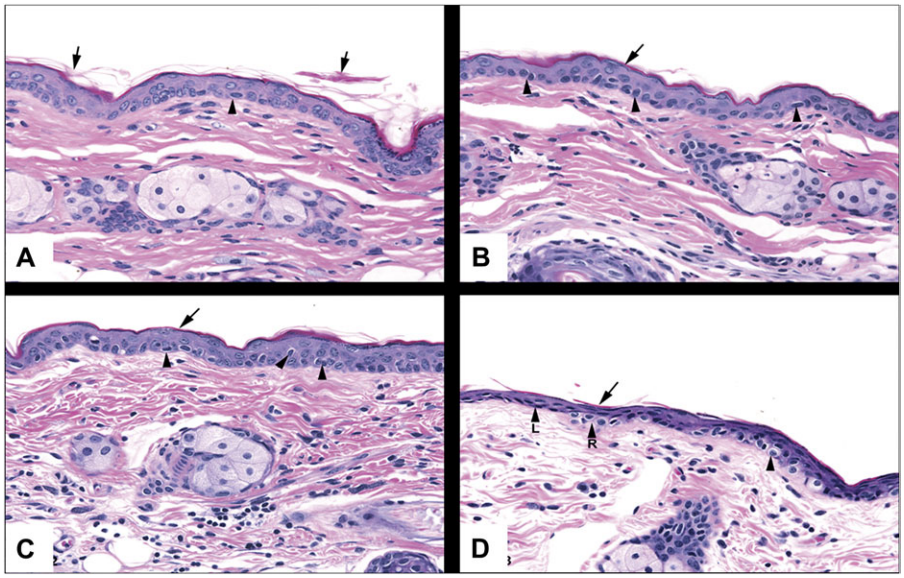

FIG. 1. Photomicrographs of skin from SKH-1 hairless mice following the application and removal of tape strips 0 (A), 5 (B), 10 (C), and 15 (D) times. The skin was stained with hematoxylin and eosin. The arrows point to partially desquamated keratin, and the arrow heads refer to cells in the stratum basale with perinuclear halos. Magnification is at ×20.

Analysis of tissues. ICP-MS was performed utilizing a Fisons PQ3 instrument (Thermo Electron Corp., Franklin, MA). Samples were prepared for analysis as previously described (Gopee *et al*., 2007) by homogenization in 18 MΩ water (Ultra-Turrax T25 homogenizer; IKA, Stauffen, Germany), and weighed portions were combined with 70% HNO_3 (Ultrex; J.T. Baker, Phillipsburg, NJ) and dissolved using microwave digestion 35 min at 300 W power, 200°C, and 220 psi (CEM, Matthews, NC) using an Xpress PTFA vessel. Recovery was established using cadmium and selenium standards (SPEX CertiPrep; Claritas, Metuchen, NJ) with quantification of ^{112}Cd, ^{114}Cd, and ^{82}Se isotopes. The limit of detection for cadmium was 3 pg/ml. The ICP-MS was optimized using ^{9}Be, ^{115}In, and ^{238}U isotope standards. The tissue levels of selenium were not used to quantify QD penetration due to the high background of naturally occurring selenium in lymph node and liver (Gopee *et al*., 2007). Calculations of the percent of administered dose (cadmium in CdSe QD) that was detected in tissues was made based on the amount of cadmium recovered in the tissues (specific activity times organ weight) divided by the administered dose (5 µl of 9.4µM QD, 18.8mM cadmium).

Microscopy. Typically, photomicrographs were obtained using bright field illumination to reveal the skin structure, using UV illumination with a filter pack to demonstrate selectively 620-nm QD fluorescent emission. Fluorescence photomicroscopy was conducted with a Leica DM RA2 photomicroscope (Leica Microsystems GmbH, Wetzlar, Germany), with bright field and fluorescence illumination, equipped with a SPOT RT-SE high resolution CCD camera/digital imaging system and SPOT imaging software (Diagnostics Instruments, Inc., Sterling Heights, MI). Filter sets for selectively visualizing 621-nm QD fluorescence utilized a 415WB/100 excitation filter, a 475DCLP dichroic filter, and 620WB20 emission filters (Omega Optical, Inc., Brattleboro, VT). Images were typically captured at ×20 and saved as a 16 BPP file.

Confocal microscopy was conducted with a Zeiss LSM 510 Meta Axiovert 200 inverted confocal microscope (Carl Zeiss, Inc., Göttingen, Germany). Images were obtained using band-pass or long-pass filters and PMT detection or the polychromatic (Meta) detector. Excitation of the QD was accomplished with a diode 405-nm laser, or the 458-, 477-, or 488-nm lines from an Argon laser. Images were viewed using the Zeiss LSM Image Browser software.

Statistical analysis. The comparison of the cadmium in the treatment groups was conducted using a one-way analysis of variance using SigmaStat software (Jandel Scientific Corp., San Rafael, CA) with pair-wise comparisons of the levels at each time and dose to the corresponding control values. Values were considered significant when the probability value was 5% or less ($p \leq 0.05$).

RESULTS

Histopathological Analysis of Mouse Skin Treatment

The question being addressed in this study was whether or not skin condition affected the dermal absorption of nanoscale materials. In this study we specifically addressed the penetration of PEG-coated QD suspended in an oil-in-water emulsion that is similar in composition to over-the-counter creams.

The preferred method for removing the stratum corneum is tape stripping, where adhesive tape is applied to the skin and following the application of constant pressure, the adhered corneocytes are removed. Rather than use existing methods from the literature, where it is difficult to match (when stated) the pressure used on the tape, we determined the number of tape strippings necessary to remove the stratum corneum from SKH-1 hairless mouse skin using a constant pressure device. The application of 5 or 10 tape stripping repetitions to the same area of skin (Fig. 1) resulted in essentially the same effect, where the superficial keratin of the stratum corneum, which was partially desquamated in control skin, had been virtually removed. The deeper keratin layer of the stratum corneum remained attached to the stratum granulosum and there was some minor, acute cellular swelling with increasing tape stripping (Fig. 1, arrow heads). When the same area of skin was subjected to 15 tape strippings, the stratum corneum had been virtually removed; however, in many of the regions where the stratum corneum appeared to be completely removed, the

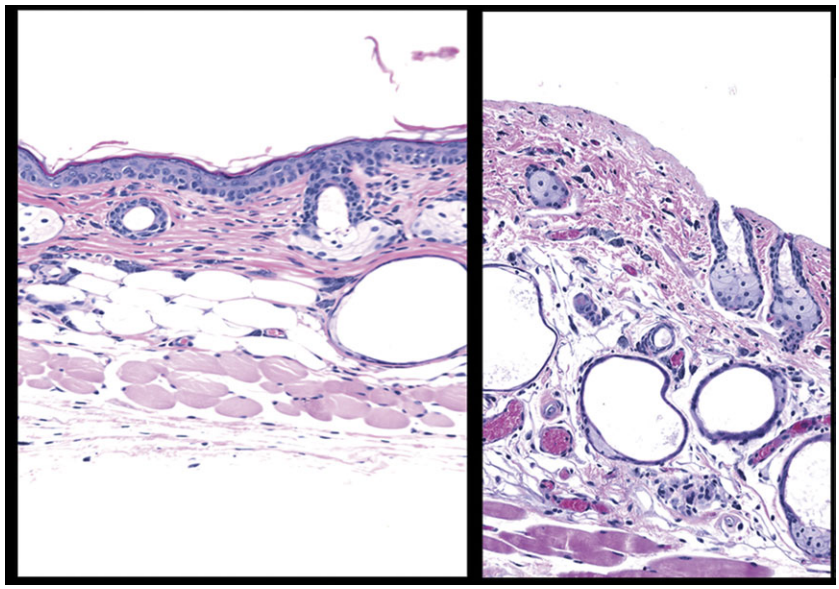

FIG. 2. Dermabrasion was used to remove the stratum corneum and epidermis. The panel on the left is skin from an untreated mouse. The skin section on the right is from a mouse where the epidermis was removed using dermabrasion (1 h prior). The skin was stained with hematoxylin and eosin. Magnification is at ×20.

epidermis stained more intensely and appeared compressed with attenuation of cellular layers (atrophy), including the stratum basale. In these regions, nuclei of cells of the stratum basale were flattened, shrunken, and hyperchromatic. As a result of the skin trauma induced by 15 tape strippings, we chose to use 10 tape strippings for the subsequent studies to achieve removal of the stratum corneum without damaging the epidermis (stratum basale and stratum granulosum).

Dermabrasion was achieved using a buffer wheel. Histopathological examination of the skin confirmed that the method led to dermabrasion (i.e., epidermal removal) and not frank injury or wounding (i.e., removal of upper dermis). As shown in Figure 2, the method resulted in the removal of the stratum corneum and the viable epidermis (two to four cell layers thick including the stratum basale). Examination of the dermis indicated that no hemorrhage was present following the dermabrasion. There was evidence of some degranulating mast cells, congested capillaries and venules, hyperemic arterioles, and margination of some neutrophils along capillary and venule endothelia. One day following the dermabrasion, the treated area was covered with a dried serum exudate (scab) and numerous inflammatory cells (image not shown), dermal inflammation, and hyperplasia of the adjacent epidermis. Three days after the dermabrasion, the treated area had a thin layer of regenerating epithelium under the scab with continued inflammation in the dermis. Complete regeneration of the epidermis occurred between days 4 and 9 (image not shown).

A group of mice was treated once daily for 4 days on a 1.6 × 1.6 cm area of skin with acetone wipes to mimic dry skin conditions. Histopathological examination of mice from this group indicated induced hyperkeratosis, parakeratosis, hyperplasia, and inflammation in the epidermis (images not shown). The most common effect in the dermis was increased thickness and density of dermal collagen (fibrosis) compared with the control.

Quantitative Distribution of QD (Cadmium) Following Application to Mice

The QD emulsion was applied to the backs of mice either intact skin or skin compromised by tape stripping, acetone

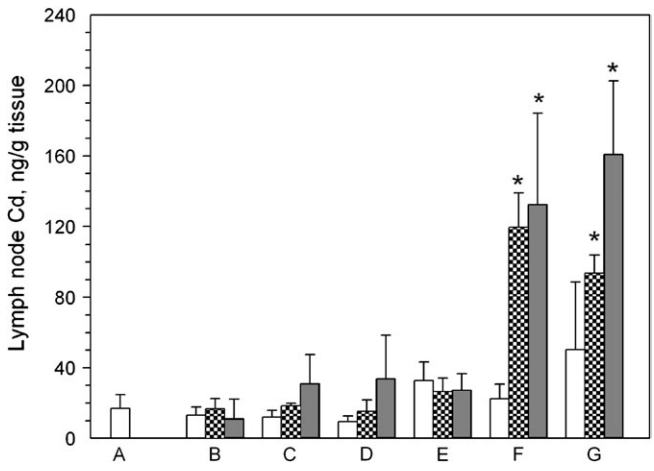

FIG. 3. Cd levels in regional lymph nodes of SKH-1 mice topically applied with CdSe QD suspended at 9μM in an oil-in-water emulsion. The axial and brachial lymph nodes were removed from mice ($n = 3$ per group) topically treated as follows: (A) no QD applied; (B) QD applied to normal skin; (C) QD applied to tape-stripped skin; (D) QD applied to acetone treated skin; (E) QD applied to untreated skin and covered with occlusion patch; (F) QD applied to dermabraded skin; (G) QD applied to dermabraded skin and covered with occlusion patch. The animals were sacrificed at 0 h (open bar), 24 h (hatched bar), or 48 h (filled bar) after application of the emulsion.

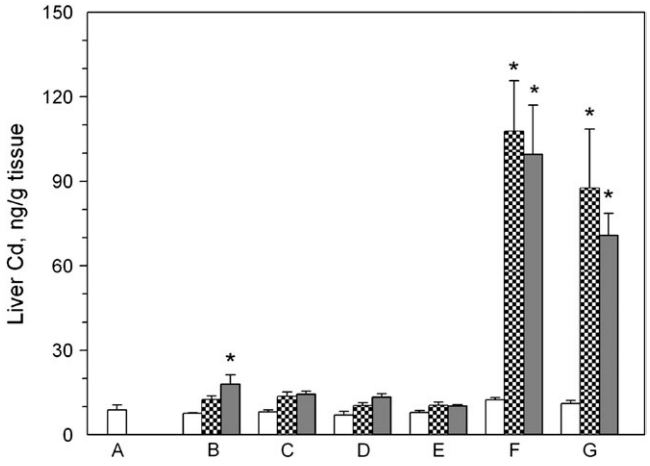

FIG. 4. Cd levels in the liver of SKH-1 mice topically applied with CdSe QD suspended at 9μM in an oil-in-water emulsion. The liver was removed from mice ($n = 3$ per group) topically treated as follows: (A) no QD applied; (B) QD applied to normal skin; (C) QD applied to tape-stripped skin; (D) QD applied to acetone treated skin; (E) QD applied to untreated skin and covered with occlusion patch; (F) QD applied to dermabraded skin; (G) QD applied to dermabraded skin and covered with occlusion patch. The animals were sacrificed at 0 h (open bar), 24 h (hatched bar), or 48 h (filled bar) after application of the emulsion.

treatment, or dermabrasion. Some of the mice in the intact or dermabraded skin groups had the site of QD application covered with an occlusion patch. At sacrifice, the liver and lymph nodes were removed and the tissue levels of cadmium (from QD) analyzed using ICP-MS as a surrogate for levels of CdSe QD within the tissue. The results of the analysis of the lymph nodes are shown in Figure 3. The application of QD to skin that was untreated (Fig. 3B) did not result in an increase in lymph node cadmium levels at 0, 24, or 48 h over the values detected in lymph nodes from control animals (Fig. 3A). Lymph node levels of cadmium were not affected at 24 or 48 h by tape strip removal of the stratum corneum (Fig. 3C), acetone pretreatment (Fig. 3D), and intact skin covered with occlusion patch (Fig. 3E). When the epidermis of the mice was removed by dermabrasion, the application of QD to the skin resulted in an increase of cadmium levels in the lymph nodes from approximately 20 ng/g tissue in the controls to approximately 120 ng/g tissue at 24 h and remained at this level at 48 h (Fig. 3F). The application of QD to dermabraded skin, and covering the application with an occlusion patch, still resulted in elevated cadmium levels in the lymph nodes at 24 and 48 h (Fig. 3G).

The levels of cadmium in the liver in the treated animals are shown in Figure 4. The application of QD to untreated skin resulted in no elevation of cadmium at 24 h (hatched bar, Fig. 4B); however, there was a statistically significant elevation at 48 h ($p < 0.05$; Fig. 4B). Liver levels of cadmium were not affected at 24 or 48 h by tape strip removal of the stratum corneum (Fig. 4C), acetone pretreatment (Fig. 4D), or intact skin covered with occlusion patch (Fig. 4E). Significant increases in liver cadmium levels were detected in the livers of mice that were treated by dermabrasion followed by application of the QD, with the cadmium increasing from approximately 20 ng/g in control and 0 h mouse livers, to approximately 100 ng/g at 24 and 48 h (Fig. 4F). The application of occlusion patches to the mice following application of QD to the dermabrasion site also resulted in increased levels of cadmium over the control at 24 and 48 h (Fig. 4G).

Considering the dose of QD applied, specific levels of Cd in the tissues, and tissue mass, the total level of cadmium detected in the livers of the dermabraded mice averaged 1.98 ± 0.08% and 1.47 ± 0.11% of the applied dose at 24 and 48 h, respectively. The application of the occlusion patch over the dermabraded area following the addition of the QD resulted in 1.96 ± 0.62% and 1.74 ± 0.06% of the applied dose in the livers at 24 and 48 h, respectively.

Fluorescence Microscopic Evidence of QD Penetration into the Skin of Dermabraded Mice

Fluorescence microscopy was used to confirm the migration of QD into the skin of mice that were dermabraded prior to the application of the QD (Fig. 5). There was an appearance of bright red fluorescence in the sections of skin from mice treated with dermabrasion (with [Fig. 5D] and without [Fig. 5F] occlusion patch) that was not present in the intact skin from control mice (Fig. 5B) or mice pretreated with tape stripping (image not shown). This red fluorescence was consistent with the emission maximum of the QD (621 nm), was concentrated in the regenerating epidermis, and was also located in the dermis and around dermal substructures. The SKH-1 mice do have some hair follicles without the development of hair shafts, and on occasion in this and other studies, we have detected QD in the upper aspects of hair follicles; however, in the dermabraded skin the penetration of the QD into the skin appeared to be independent of the presence of follicles, and QD penetration was a general phenomenon in the dermabraded skin.

Further evidence that the QD migrated into the dermis following application of QD to dermabraded skin was provided by confocal microscopy with polychromatic detection. QD fluorescence was visible in the dermis using confocal microscopy with fluorescence detection and a > 575-nm long-pass filter (Fig. 6B). The QD are highly visible on the surface of the dermabraded skin (left aspect of Fig. 6B) with QD fluorescence apparent in the dermis and especially in two areas below the epidermis (middle and right sides of Fig. 6B). Autofluorescence in mouse, pig, and human skin typically is detected in the light passed by the 505- to 550-nm band-pass filter and > 575 nm long-pass filter. The wavelength of the fluorescence in the dermis following application of QD to dermabraded skin was > 575 nm (Fig. 6B), but not present in the 505- to 550-nm band-pass window (Fig. 6A) suggesting the fluorescence was the result of the presence of the QD (621 nm emission). A composite of the images in Figures 6A-C is shown as Figure 6D, revealing dermis structural aspects and the location of the QD.

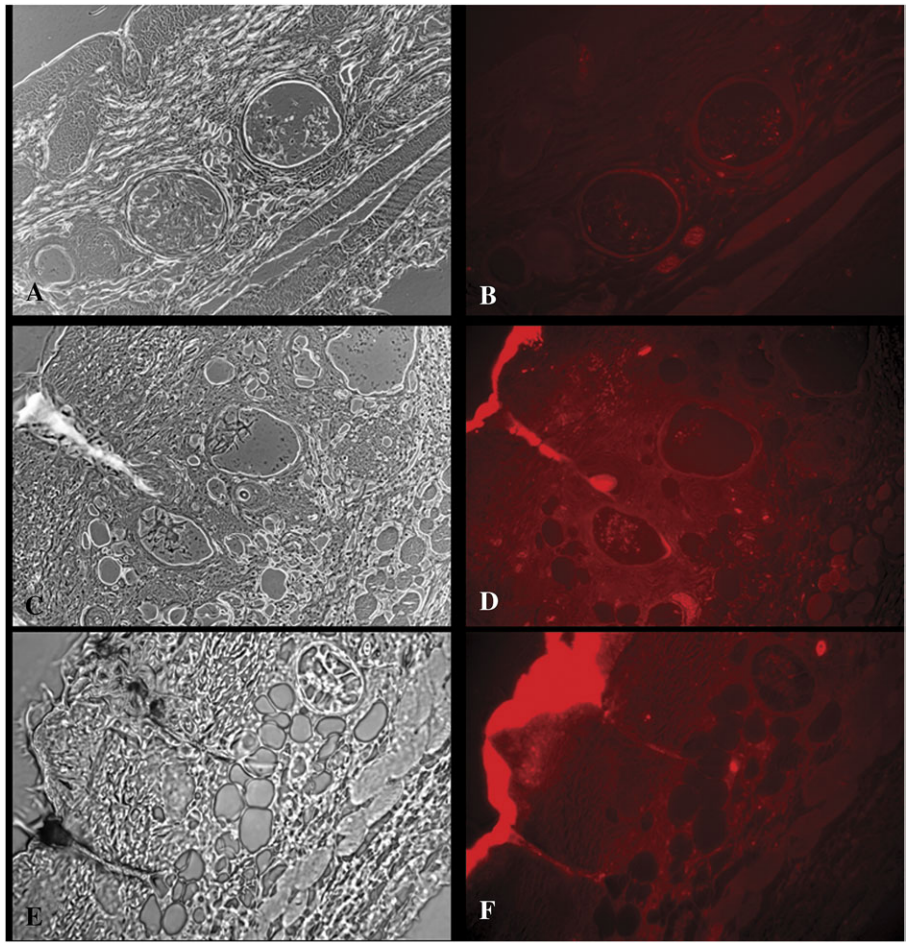

FIG. 5. Photomicroscopic bright field (A, C, E) and fluorescence (B, D, F) images of intact skin (A, B), and dermabraded skin with (C, D) and without an occlusion patch (E, F) 48 h after topical application of QD. The epidermis is in the upper left corner of each image. The QD, which emit fluorescence at 621 nm, appear red in the images.

The tissue section shown in Figure 6 was reexamined using confocal fluorescence microscopy and spectral analysis of the fluorescence emissions. Figure 7 shows the fluorescence image of the dermabraded skin following QD application (upper image, Fig. 7), and the spectral analysis of the fluorescence in four specific areas of the slide. Area A, Figure 7, is the upper aspects of the dermabraded skin where the QD concentrated following application. The spectrum of the fluorescence emission at a pixel in the center of area A is shown as spectrum A. The fluorescence emission has a sharp peak centered at 620 nm as would be expected for the QD (621-nm emission maximum). Autofluorescence routinely seen in skin does not have a sharp emission peak (spectrum not shown), and has a pattern of emission peaks at ~600, ~630, and ~680 nm with intensities considerably less than those of the QD. Similarly, the spectrum for the fluorescence detected at representative pixels in areas B, C, and D, Figure 7, have fluorescence spectral emissions at 620 nm, which is consistent with the fluorescence emission from the QD. Examinations of the fluorescence spectral in the dermis from other dermabraded and control tissues following treatment with QD resulted in the same conclusion, that is, that the QD were penetrating dermabraded skin and not control or tape-stripped skin.

DISCUSSION

In this study, we describe the penetration of nanoparticles (QD) through skin *in vivo* following application in a cream similar to those used in skin lotions or sunscreens. The PEG-coated QD were topically applied at a dose of 9.4μM at a cream dose rate of 2 mg/cm^2. When the QD were applied to intact skin or skin where the stratum corneum was removed by tape stripping, we found no evidence of the migration of the QD into and through the skin to the regional lymph nodes or liver, based on the measurement of cadmium in tissues and fluorescent QD by confocal microscopy. We did detect elevated cadmium in the liver from one group of mice at 48 hr after application of QD to intact skin. However, taking

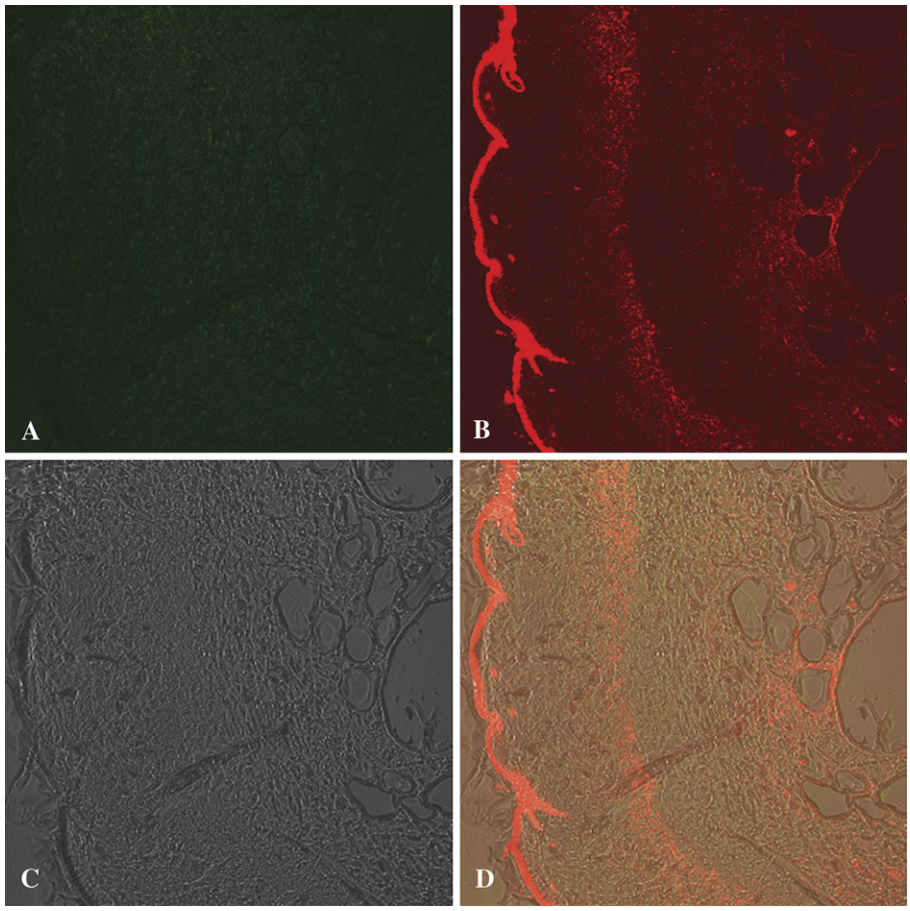

FIG. 6. Representative images generated by confocal fluorescence microscopy are shown of dermabraded skin treated for 24 h with QD. The upper left image (A) was taken using a band-pass filter (505–550 nm) allowing collection of autofluorescence, whereas the upper right image (B) was taken using a long-pass filter (> 575 nm) which would contain the target QD (fluorescence emission at 621 nm). The lower left panel (C) shows the differential interference contrast image (Nomarski interference contrast) image of the skin, and the lower right image (D) is a composite of images (A–C).

into consideration the lack of significant increase of cadmium in the lymph nodes and liver of other groups (e.g., tape stripped, acetone treated, intact skin covered with occlusion patch), we conclude that this one result is probably spurious and that there is no evidence of QD penetration through skin containing an intact epidermis and biodistribution to the lymph nodes or liver. The same cannot be said for application of the QD to the skin of animals that had the skin damaged through dermabrasion. We found a significant increase in the level of cadmium in the lymph nodes and livers of mice pretreated with dermabrasion. Considering the amount of cadmium contained in the applied QD, we were able to detect the migration of 1.98 and 1.96% of the topically applied dose in the livers in 24 h in dermabraded skin with and without the occlusion patch, respectively. This also indicates that of the approximately 2.8×10^{13} QD that were applied to the mice, approximately 5.6×10^{11} penetrated the skin and migrated to the liver. To the best of our knowledge, this is the first quantitative determination of the migration of QD from the skin into internal sentinel organs.

Tape stripping is the most common method to remove the outermost barrier of the skin to environment. Studies have shown that the greater the number of tape strippings can increase the degree of corneocyte removal and epidermis damage can occur; however, these results are dependent on the tape, pressure, and time on the skin (Breternitz *et al*., 2007). As an example, Oudshoorn *et al*. (2009) have shown that the application of four tape strippings with fingertip pressure to SKH-1 mice resulted in transepidermal water loss (TEWL), but not complete removal of corneocytes. After six, seven, and eight tape strippings, the TEWL was increased, and the corneocyte removal was complete at eight tape strippings. With eight or less tape strippings the skin recovered within 24 or 48 h, however, with 12 tape strippings, the skin was damaged to the point that it did not recover in 48 h. In our study we quantified the number of tape strips required to achieve stratum corneum removal without damaging the epidermis using histology. Our results that 10 tape strippings are adequate are consistent with those of Oudshoorn *et al*. (2009).

In a prior study we established that the lymph nodes and liver were appropriate sentinel organs for distribution of PEG-coated QD (37 nm diameter) following intradermal injection (Gopee *et al*., 2007). The QD disbursed throughout the viable

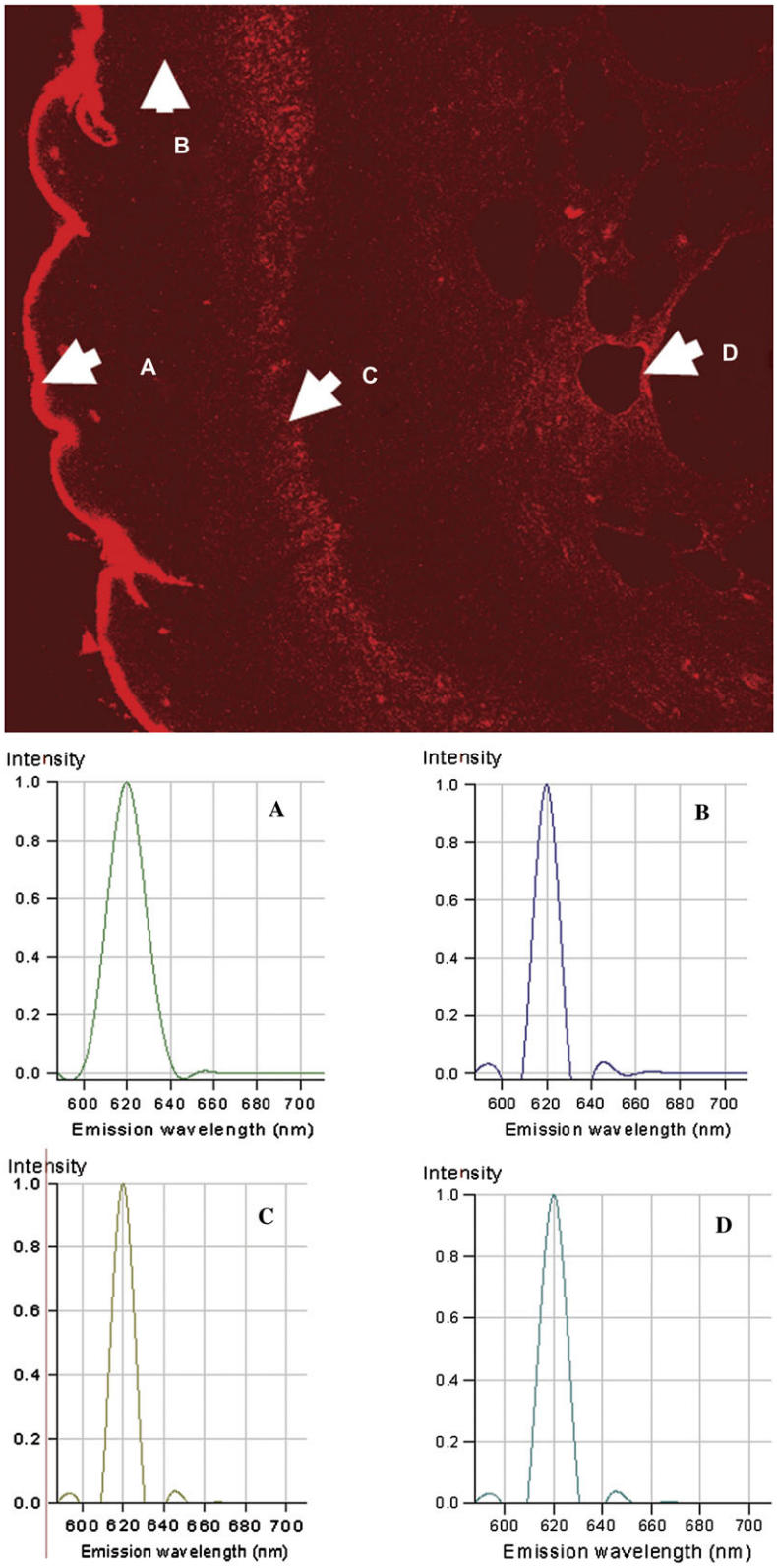

FIG. 7. The fluorescence spectra in the indicated areas (A–D) of the representative tissue sample were determined using the spectrum analysis component of the confocal fluorescence microscope. The spectra for each of the points (A–D) indicated in the figure are shown in the lower spectral plots. Point-A is of QD on the stratum corneum, and had maximum fluorescence at 620 nm. Similarly, fluorescence in areas (B–D) in the dermis had spectra indicative of the 621-nm QD.

subcutis at the injection site (visualized using fluorescence microscopy) and were additionally visible within minutes migrating through the lymphatics to the regional draining lymph nodes (Gopee *et al*., 2007). The migration of the QD was quantitatively determined using ICP-MS and was based on the cadmium content of the CdSe-based QD. At 24 h following injection, approximately 6% of the injected dose of QD was contained in the liver, with ~1 and ~0.5% present in the regional lymph nodes and kidney, respectively. This study established that if PEG-coated QD were present in the dermis, the migration of the QD from the dermis could be monitored using the regional draining lymph nodes, liver, and kidney as sentinel organs. These results were very similar to those reported by Manolova *et al*. (2008) following injection of virus-like particles (30 nm) and polystyrene spheres (20, 500, 1000, and 2000 nm). They found that the 20-nm virus-like particles and 20-nm polystyrene spheres migrated from the footpad (injection site) to the popliteal lymph nodes by free drainage and were taken up by macrophages, whereas the larger polystyrene spheres (500–2000 nm) were transported to the lymph nodes by dendritic cells. Fluorescence microscopic analysis of tissue sections revealed a similar pattern of initial deposition of free nanoparticles through the lymph system to the sinuses (Fig. 2, Gopee *et al*., 2007; Fig. 2, Manolova *et al*., 2008) where they interact with either subcapsular macrophages or lymph node resident $CD8\alpha^{+}$ dendritic cells.

The skin can be a difficult organ in which to assess penetration of drugs and materials; however, because the skin is an important first line of defense against many environmental and topically applied materials, it is very important to understand its potential as a barrier, especially to nanoscale materials. As a result, several methods have been developed to assess epidermal penetration and possible distribution to the rest of the body of drugs and chemicals: (1) application to skin *in vitro* and examination of skin for test material or flow-through fluid for test article; (2) application to skin *in vivo* and detection of the test material either (a) in the skin or (b) in sentinel organs following biodistribution.

The first method for determining skin penetration, an *in vitro*–based method, involves removal of the skin from an animal, the skin is stretched over a holding apparatus (e.g., flow-through diffusion cell; Bronaugh, 2000; Bronaugh and Stewart, 1985), the test article applied to the epidermis side of the skin, and penetration is assessed by detecting nanoparticle presence in the epidermis or dermis, or by detection of the nanoparticle in the fluid that passed underneath the skin. Baroli *et al*. (2007) studied the penetration of nanoscale tetramethylammonium hydroxide stabilized maghemite (6 nm) and sodium bis(2-ethylhexyl)sulfosuccinate stabilized iron (predominantly 5 nm) as aqueous suspensions in a diffusion cell *in vitro* using full thickness human skin. Skin samples were exposed to the nanoparticles and removed, frozen, and analyzed using scanning electron microscopy with backscatter electron imaging and energy dispersive X-ray analysis (EDS). Using this method, the authors were able to demonstrate that the iron nanoparticles were contained in the stratum corneum, sometimes in the uppermost sections of the viable epidermis, and in rare cases below the stratum corneum and epidermal junction. This study clearly demonstrated the integrity of the skin barrier to a particular nanoparticle, but also demonstrated the necessity of robust methods to analyze the skin for nanoparticles (e.g., EDS).

Tinkle and colleagues (Tinkle *et al*., 2003) used human skin samples, and determined the penetration of 0.5-, 1-, 2-, or 4-μm-diameter fluorescent dextran spheres into the skin following continual skin flexing (45°, 0.33 Hz). Sections of the skin were analyzed using confocal fluorescence microscopy for fluorescence particle penetration. The 0.5- and 1-μm beads penetrated to the stratum corneum and epidermal interface, with some particles penetrating into the epidermis after 30 and 60 min. Most notable, discontinuous stratum corneum allowed significantly more penetration of the particles into the epidermis.

In another study, gold nanoparticles (15, 102, and 198 nm) were suspended in 0.15M phosphate, pH 7.4, were applied to rat skin using the *in vitro* skin system (e.g., Franz diffusion cell) and quantified using electron microscopy with X-ray energy dispersive spectrometry (Sonavane *et al*., 2008). In 24 h, the 15-nm gold penetrated the skin to an extent that was ~125 and ~3800 times greater that of the 102- and 198-nm gold, respectively. Using constantly perfused rat intestine, at 6 h the 15-nm gold had permeated the intestines to an extent that was ~75 and ~980 times greater than the 102 and 198-nm gold, respectively.

In a study by Ryman-Rasmussen *et al*. (2006), commercially available QD were applied to porcine skin using an *in vitro* flow-through diffusion cell. The QD were PEG coated (35 and 45 nm), PEG-coated amine terminated (15 and 20 nm), or PEG-coated carboxylic acid terminated (14 and 18 nm) and suspended in a borate buffer. After application, a physiological-equivalent perfusate was applied to facilitate diffusion into and through the skin. Using confocal microscopy the authors demonstrated that PEG-coated QD penetrated the intact stratum corneum and into the epidermis (Ryman-Rasmussen *et al*., 2006). The amine terminated QD penetrated the stratum corneum into the epidermis, and some were found in the dermis by 8 h. The carboxylic acid terminated QD remained in the stratum corneum at 8 h, with some evidence of penetration at 24 h. These studies were extended, applying the same PEG-coated QD as used in the current study as an aqueous suspension to porcine skin *in vitro* (Zhang *et al*., 2008b). Using confocal fluorescence microscopy, the QD did not penetrate the stratum corneum or were found at the stratum corneum stratum granulosum interface, but were not detected in the epidermis.

Together the studies of Tinkle *et al*. (2003), Ryman-Rasmussen *et al*. (2006), Baroli *et al*. (2007), Zhang *et al*. (2008b), Rouse *et al*. (2007) using fullerene derivatized peptides, and Sonavane *et al*. (2008) demonstrate that

nanoparticle penetration of skin is dependent on the particle size and chemistry, and that assumptions should not be made regarding skin penetration by nanomaterials. In addition, the power of the observations and conclusions regarding skin penetration is dependent on the methodology used to analyze the samples for the nanoparticles, where methods such as EDS show a tremendous ability to qualitatively measure the penetration of nanoparticles into skin. The studies by Tinkle *et al*. (2003) suggested that skin integrity might provide a route of entry of particles into the epidermis.

Our results, showing that a significant percentage of the dose of topically applied QD penetrated the skin following damage (e.g., dermabrasion) and migrated to the lymph nodes and liver, is consistent with recent observations by others. Zhang and Monteiro-Riviere (2008) applied an aqueous solution of commercially available QD to rat skin (hair clipped) that was either tape stripped or abraded by sandpaper. The penetration of the QD into the skin was assessed using confocal microscopy and there was no evidence of epidermal penetration following tape stripping; however, abrasion using sandpaper led to penetration of the QD into the dermis (Zhang and Monteiro-Riviere, 2008). Our results using confocal fluorescence microscopy are consistent with those of Zhang and Monteiro-Riviere (2008), but more importantly, reinforce their microscopic observations of QD in the skin, by detecting and quantifying the distribution of QD to regional lymph nodes and liver. Zhang and Monteiro-Riviere (2008) replicated the *in vitro* skin flexing studies reported by Tinkle *et al*. (2003) using PEG-coated QD and rat skin. They were not able to visualize QD penetrating into the viable epidermis following 60 min of flexing.

In a recent study, Mortensen *et al*. (2008) applied carboxylic acid terminated PEG-coated QD in a 75% glycerol solution to the backs of hairless mice. The mouse skin was either normal or pretreated 1 h prior with an erythemic dose of UV (270 mJ/cm^2 UVB). Using confocal fluorescence microscopy and narrow band-pass filters, Mortensen *et al*. (2008) demonstrated low levels of QD penetration through the stratum corneum and into the epidermis of skin from control mice at 24 h, and the effect of ultraviolet light was to increase the extent of penetration. The presence of the QD in the epidermis was confirmed using transmission electron microscopy with EDS.

Our observations along with those of Zhang and Monteiro-Riviere (2008) and Mortensen *et al*. (2008) demonstrate that damaged skin (either dermabrasion or UV-induced damage) could be a portal for entry of nanoparticles into the viable epidermis and dermis, and our studies extend these observations to show that the penetrating particles can biodistribute to other organs, thereby increasing the exposure and potential for adverse effects.

In conclusion, we were able to quantify the dermal penetration of PEG-coated QD nanoparticles into and through the skin of mice following skin damage (removal of epidermis, dermabrasion). Skin penetration did not occur in mouse skin (which is considerably thinner than human skin) when the skin was untreated, when the stratum corneum was removed by tape stripping, or when the skin was pretreated with acetone (dry skin). Skin penetration did not occur in The QD biodistributed and were detected in the regional lymph nodes and liver. We propose that proper assessment of the dermal penetration of nanoparticles should require quantitative determination of the distribution of the nanoparticles to internal organs (e.g., sentinel lymph nodes and liver) in addition to the examination of the presence of nanoparticles in the skin (see Baroli *et al*., 2007; Zhang *et al*., 2008b). In order to conduct proper risk assessments for dermal exposure to nanomaterials, in addition to knowing the toxicity of the nanoparticles, the condition of the skin and the internalization of the nanoparticles need to be quantified.

FUNDING

Interagency agreement (IAG 224-93-001) between the U.S. Food & Drug Administration and the National Institute of Environmental Health Sciences (NIEHS), National Institutes of Health (NIH), and in part by the Intramural Research Program of the NIEHS/NIH; and University of Arkansas for Medical Sciences Digital and Confocal Microscopy Laboratory supported by NIH Grant (2 P20 RR 16460) (L. Cornett, PI, INBRE, Partnerships for Biomedical Research in Arkansas) and NIH/NCRR Grant (1 S10 RR 19395) (R. Kurten, PI, ''Zeiss LSM 510 META Confocal Microscope System'').

ACKNOWLEDGMENTS

The authors would also like to acknowledge use of the National Institute of Environmental Health Sciences (NIEHS) Confocal Microscope Facility. The authors would like to acknowledge C.S. Trempus (NIEHS) for providing guidance on the dermabrasion, and S.S. Tinkle and M.F. Cesta (NIEHS) for reviewing the manuscript. The contents of this manuscript do not necessarily reflect the views and policies of the U.S. Food & Drug Administration, National Toxicology Program, NIEHS, or NIH. The mention of trade names or commercial products does not constitute endorsement or recommendation for use.

REFERENCES

Alekseenko, A. V., Waseem, T. V., and Fedorovich, S. V. (2008). Ferritin, a protein containing iron nanoparticles, induces reactive oxygen species formation and inhibits glutamate uptake in rat brain synaptosomes. *Brain Res.* **1241,** 193–200.

Arakaki, A., Nakazawa, H., Nemoto, M., Mori, T., and Matsunaga, T. (2008). Formation of magnetitie by bacteria and its application. *J. R. Soc. Interface* **5,** 977–999.

Bailey, R. (2003). The smaller the better: the limitless promise of nanotechnology and the prowing peril of a moratorium. ReasonOnline. Available at: www.reason.com/news/show/28969.html. Accessed March 13, 2009.

Baroli, B., Ennas, M. G., Loffredo, F., Isola, M., Pinna, R., and López-Quintela, M. A. (2007). Penetration of metallic nanoparticles in human full-thickness skin. *J. Invest. Dermatol.* **127,** 1701–1712.

Bhattacharya, P., Ghosh, S., and Stiff-Roberts, A. D. (2004). Quantum dot opto-electronic devices. *Annu. Rev. Mater. Res.* **34,** 1–40.

Breternitz, M., Flach, M., Prassler, J., Elsner, P., and Fluhr, J. W. (2007). Acute barrier disruption by adhesive tapes is influenced by pressure, time, and anatomical location: Integrity and cohesion assessed by sequential tape stripping. A randomized controlled study. *Br. J. Dermatol.* **156,** 231–240.

Bronaugh, R. L. (2000). *In vitro* percutaneous absorption models. *Ann. N. Y. Acad. Sci.* **919,** 188–191.

Bronaugh, R. L., and Stewart, R. F. (1985). Methods for *in vitro* percutaneous absorption studies IV: The flow-through diffusion cell. *J. Pharm. Sci.* **74,** 64–67.

Busek, P. R. (2002). Geological fullerenes: review and analysis. *Earth Planet. Sci. Lett.* **203,** 781–792.

Busek, P. R., Tsipursky, S. J., and Hettich, R. (1992). Fullerenes for the geological environment. *Science* **257,** 215–217.

Çiftçioğlu, N., Vejdani, K., Lee, O., Mathew, G., Aho, K. M., Kajander, E. O., McKay, D. S., Jones, J. A., and Stoller, M. L. (2008). Association between Randall's plaque and calcifying nanoparticles. *Int. J. Nanomed.* **3,** 105–115.

Dobson, R. L., Motlagh, S., Quijano, M., Cambron, R. T., Baker, T. R., Pullen, A. M., Regg, B. T., Bigalow-Kern, A. S., Vennard, T., Fix, A., *et al.* (2008). Identification and characterization of toxicity of contaminants in pet food leading to an outbreak of renal toxicity in cats and dogs. *Toxicol. Sci.* **106,** 251–262.

ETC, Action group on Erosion, Technology, and Concentration. (2003). Size matters! ETC group: New information provides more evidence for mandatory moratorium on synthetic nanoparticles. News release, 14 April 2003. A vailable at www.etcgroup.org/en/materials.publications.html?pub_id=164. Accessed February 26, 2009.

ETC, Action group on Erosion, Technology, and Concentration. (2006). Nanotech product recall underscores need for nanotech moratorium. New release, 7 April 2006. Available at www.etcgroup.org/en/materials.publications.html?pub_id=14. Accessed February 26, 2009.

Feynman, R. P. (1959). There's plenty of room at the bottom. Lecture delivered 29 Dec 1959, at annual meeting of Am. Phys. Soc. Available at http://www.zyvex.com/nanotech/feynman.html. Accessed February 26, 2009.

Gao, X., Yang, L., Petros, J. A., Marshall, F. F., Simons, J. W., and Nie, S. (2005). In vivo molecular and cellular imaging with quantum dots. *Curr. Opin. Biotechnol.* **16,** 63–72.

Gopee, N. V., Roberts, D. W., Webb, P., Cozart, C. R., Siitonen, P. H., Warbritton, A. R., Yu, W. W., Colvin, V. L., Walker, N. J., and Howard, P. C. (2007). Migration of intradermally injected quantum dots to sentinel organs in mice. *Toxicol. Sci.* **98,** 249–257.

Hansen, S. F., Michelson, E. S., Kamper, A., Borling, P., Stuer-Lauridsen, F., and Baun, A. (2008). Categorization framework to aid exposure assessment of nanomaterials in consumer products. *Ecotoxicology* **17,** 438–447.

Kim, J. S., Kuk, E., Yu, K. N., Kim, J. H., Park, S. J., Lee, H. J., Kim, S. H., Park, Y. K., Park, Y. H., Hwang, C. Y., *et al.* (2007). Antimicrobial effects of silver nanoparticles. *Nanomedicine* **3,** 95–101.

Knight, A., Gaunt, J., Davidson, T., Chechik, V., and Windsor, S. (2004). Evaluation of the stability of quantum dots as fluorescence standards. NPL Report DQL-AS 007.

Komeili, A. (2007). Molecular mechanisms of magnetosome formation. *Annu. Rev. Biochem.* **76,** 351–366.

Lee, J.-H., Huh, Y.-M., Jun, Y.-W., Seo, J.-W., Jang, J.-T., Song, H.-T., Kim, S., Cho, E.-J., Yoon, H.-G., Suh, J.-S., *et al.* (2007). Artificially engineered magnetic nanoparticles for ultra-sensitive molecular imaging. *Nat. Med.* **13,** 95–99.

Les, C. B. (2008). Quantum dots point to a $721.1 million market. Available at: Photonics.com; http://www.photonics.com/printerFriendly.aspx?ArticleID=35500&Publication=5. Accessed March 10, 2009.

Li, Q., Mahendra, S., Lyon, D. Y., Brunet, L., Liga, M. V., Li, D., and Alvarez, P. J. (2008). Antimicrobial nanomaterials for water disinfection and microbial control: Potential applications and implications. *Water Res.* **42,** 4591–4602.

Longmire, M., Choyke, P. L., and Kobayahsi, H. (2008). Clearance properties of nano-sized particles and molecules as imaging agents: Considerations and caveats. *Nanomedicine* **3,** 703–717.

Luoma, S. N. (2008). Silver nanotechnologies and the environment: Old problems or new challenges? Woodrow Wilson International Center for Scholars, Project on Emerging Technologies, and PEW Charitable Trusts publication PEN15. Available at: http://www.nanotechproject.org/publications/archive/silver/. Accessed March 12, 2009.

Manolova, V., Flace, A., Bauer, M., Schwarz, K., Saudan, P., and Bachmann, M. F. (2008). Nanoparticles target distinct dendritic cell populations according to their size. *Eur. J. Immunol.* **38,** 1404–1413.

Miller, G. (2008). Mounting evidence that carbon nanotubes may be the new asbestos. Friends of the Earth Australia. Available at: www.nano.foe.org.au/filestone2/download/265/Mounting%20evidence%20that%20carbon%20nanotubes%20may%20be%20the%20new%20asbestos%20=%20August%202008.pdf. Accessed February 26, 2009.

Minetti, C. A., and Remeta, D. P. (2006). Energetics of membrane protein folding and stability. *Arch. Biochem. Biophys.* **453,** 32–53.

Mortensen, L. J., Oberdörster, G., Pentland, A. P., and DeLouise, L. A. (2008). *In vivo* skin penetration of quantum dot nanoparticles in the murine model: The effect of UVR. *Nano Lett.* **8,** 2779–2787.

Mossman, D., Eigendorf, G., Tokaryk, D., Gauthier-Lafaye, F., Guckert, K. D., Melezhik, V., and Farrow, C. E. G. (2003). Testing of fullerenes in geologic materials: Oklo carbonaceous substances, Karelian shungites, Sudbury Black Tuff. *Geology* **31,** 255–258.

National Cancer Institute (NCI). NCI Alliance for Nanotechnology in Cancer (http://nano.cancer.gov), NCI Nanotechnology Characterization Laboratory (http://ncl.cancer.gov/). Accessed February 12, 2009.

National Institutes of Health (NIH). NIH Roadmap for Medical Research (http://nihroadmap.nih.gov/nanomedicine/index.asp), National Institute of Biomedical Imaging and Bioengineering (http://www.nibib.nih.gov/Research/NIH Nano). Accessed February 12, 2009.

National Nanotechnology Initiative (NNI) http://www.nano.gov. Accessed February 12, 2009.

Nirmal, M., Dabbousi, B. O., Bawendi, M. G., Macklin, J. J., Trautman, J. K., Harris, T. D., and Brus, L. E. (1996). Fluorescence intermittency in single cadmium selenide nanocrystals. *Nature* **383,** 802–804.

Nohynek, G. J., Dufour, E. K., and Roberts, M. S. (2008). nanotechnology, cosmetics and the skin: Is there a health risk? *Skin Pharmacol. Physiol.* **21,** 136–149.

Nohynek, G. J., Lademann, J., Ribaud, C., and Roberts, M. S. (2007). Grey Goo on the skin? Nanotechnology, cosmetic and sunscreen safety. *Crit. Rev. Toxicol.* **37,** 251–277.

Oberdörster, G., Oberdörster, E., and Oberdörster, J. (2005). Nanotoxicology: An emerging discipline evolving from studies of ultrafine particles. *Environ. Health Perspect.* **113,** 823–839.

Oudshoorn, M. H. M., Rissmann, R., van der Coelen, D., Hennick, W. E., Ponec, M., and Bouwstra, J. A. (2009). Development of a murine model to evaluate the effect of vernix caseosa on skin barrier recovery. *Exp. Dermatol.* **18,** 178–184.

Rai, M., Yadav, A., and Gade, A. (2009). Silver nanoparticles as a new generation of antimicrobials. *Biotechnol. Adv.* **27,** 76–83.

Reimann, S. M., and Manninen, M. (2002). Electronic structure of quantum dots. *Rev. Modern Phys.* **74,** 1283–1342.

Reimschuessel, R., Gieseker, C. M., Miller, R. A., Ward, J., Boehmer, J., Rummel, N., Heller, D. N., Nochetto, C., de Alwis, G. K., Bataller, N., *et al.* (2008). Evaluation of the renal effects of experimental feeding of melamine and cyanuric acid to fish and pigs. *Am. J. Vet. Res.* **69,** 1217–1228.

Robertson, W. G. (2004). Kidney models of calcium oxalate stone formation. *Nephron. Physiol.* **98,** 21–30.

Rouse, J. G., Yang, J., Ryman-Rasmussen, J. P., Barron, A. R., and Monteiro-Riviere, N. A. (2007). Effects of mechanical flexion on the penetration of fullerene amino acid-derivatized peptide nanoparticles through skin. *Nano Lett.* **7,** 155–160.

Ryman-Rasmussen, J. P., Riviere, J. E., and Monteiro-Riviere, N. A. (2006). Penetration of intact skin by quantum dots with diverse physiochemical properties. *Toxicol. Sci.* **91,** 159–165.

Schneider, D., Finger, C., Prodöhl, A., and Volker, T. (2007). From interactions of single transmembrane helices to folding of alpha-helical membrane proteins: Analyzing transmembrane helix-helix interactions in bacteria. *Curr. Protein Pept. Sci.* **8,** 45–61.

Sonavane, G., Tomoda, K., Sano, A., Ohshima, H., Terada, H., and Makino, K. (2008). In vitro permeatoin of gold nanoparticles through rat skin and rat intestine: Effect of particle size. *Colloids Surfaces B Biointerfaces* **65,** 1–10.

Sosnovik, D. E. (2008). Molecular imaging in cardiovascular magnetic resonance imaging: Current perspective and future potential. *Top. Magn. Reson. Imaging* **19,** 59–68.

Theil, E. C., Matzapetakis, M., and Liu, X. (2006). Ferritins: Iron/oxygen biominerals in protein nanocages. *J. Biol. Inorg. Chem.* **11,** 803–811.

Tinkle, S. S., Antonini, J. M., Rich, B. A., Roberts, J. R., Salmen, R., DePree, K., and Adkins, E. J. (2003). Skin as a route of exposure and sensitization in chronic beryllium disease. *Environ. Health Perspect.* **111,** 1202–1208.

Trempus, C. S., Mahler, J. F., Ananthaswamy, H. N., Loughlin, S. M., French, J. E., and Tennant, R. W. (1998). Photocarcinogenesis and susceptibility to UV radiation in the v-Ha-*ras* transgenic Tg.AC mouse. *J. Invest. Dermatol.* **111,** 445–451.

Westhof, E., and Hardy, N. (2004). Folding and self-assembly of biological macromolecules. In *Proceedings of the Deuxièmes Entretiens de Bures* (E. Westhof and N. Hardy, Eds.), pp. 399. ISBN 9812385002. World Scientific Publishing Co., Inc., Hackensack, NJ.

White, S. H., and Wimley, W. C. (1999). Membrane protein folding and stability: Physical principles. *Annu. Rev. Biophys. Biomol. Struct.* **28,** 319–365.

Whitesides, G. M., Mathias, J. P., and Seto, C. T. (1991). Molecular self-assembly and nanochemistry: A chemical strategy for the synthesis of nanostructures. *Science* **254,** 1312–1319.

Woodrow Wilson Institute for Scholars, Project on Emerging Nanotechnologies. Available at: http://www.nanotechproject.org/inventories/consumer/. Text searched for "silver". Accessed December 1, 2008.

Zhang, L. W., and Monteiro-Riviere, N. A. (2008). Assessment of quantum dot penetration into intact, tape- = stripped, abraded and flexed rat skin. *Skin Pharmacol. Physiol.* **21,** 166–180.

Zhang, L. W., Yu, W. W., Colvin, V. L., and Monteiro-Riviere, N. A. (2008). Biological interactions of quantum dot nanoparticles in skin and in human epidermal keratinocytes. *Toxicol. Appl. Pharmacol.* **228,** 200–211.

Zheng, J., Nicovich, P. R., and Dickson, R. M. (2007). Highly fluorescent noble-metal quantum dots. *Annu. Rev. Phys. Chem.* **58,** 409–431.

Zlotnick, A. (2005). Theoretical aspects of virus capsid assembly. *J. Mol. Recog.* **18,** 479–490.